

Precise Measurement of the CP Violation Parameter $\sin 2\phi_1$ in $B^0 \rightarrow (c\bar{c})K^0$ Decays

I. Adachi,⁹ H. Aihara,⁴⁹ D. M. Asner,³⁷ V. Aulchenko,¹ T. Aushev,¹⁴ T. Aziz,⁴⁴ A. M. Bakich,⁴³ A. Bay,²¹ V. Bhardwaj,²⁹ B. Bhuyan,¹⁰ M. Bischofberger,²⁹ A. Bondar,¹ A. Bozek,³² M. Bračko,^{24,15} T. E. Browder,⁸ P. Chen,³¹ B. G. Cheon,⁷ K. Chilikin,¹⁴ R. Chistov,¹⁴ K. Cho,¹⁸ S.-K. Choi,⁶ Y. Choi,⁴² J. Dalseno,^{25,45} M. Danilov,¹⁴ Z. Doležal,² Z. Drásal,² S. Eidelman,¹ D. Epifanov,¹ J. E. Fast,³⁷ V. Gaur,⁴⁴ N. Gabyshev,¹ A. Garmash,¹ Y. M. Goh,⁷ B. Golob,^{22,15} J. Haba,⁹ K. Hara,⁹ T. Hara,⁹ K. Hayasaka,²⁸ H. Hayashii,²⁹ T. Higuchi,⁹ Y. Horii,²⁸ Y. Hoshi,⁴⁷ W.-S. Hou,³¹ Y. B. Hsiung,³¹ H. J. Hyun,²⁰ T. Iijima,^{28,27} A. Ishikawa,⁴⁸ R. Itoh,⁹ M. Iwabuchi,⁵⁵ Y. Iwasaki,⁹ T. Iwashita,²⁹ T. Julius,²⁶ P. Kapusta,³² N. Katayama,⁹ T. Kawasaki,³⁴ H. Kichimi,⁹ C. Kiesling,²⁵ H. J. Kim,²⁰ H. O. Kim,²⁰ J. B. Kim,¹⁹ J. H. Kim,¹⁸ K. T. Kim,¹⁹ Y. J. Kim,¹⁸ K. Kinoshita,³ B. R. Ko,¹⁹ S. Koblitz,²⁵ P. Kodyš,² S. Korpar,^{24,15} P. Križan,^{22,15} P. Krokovny,¹ T. Kuhr,¹⁷ R. Kumar,³⁸ T. Kumita,⁵¹ A. Kuzmin,¹ Y.-J. Kwon,⁵⁵ J. S. Lange,⁴ S.-H. Lee,¹⁹ J. Li,⁴¹ Y. Li,⁵³ C. Liu,⁴⁰ Y. Liu,³¹ Z. Q. Liu,¹¹ D. Liventsev,¹⁴ R. Louvot,²¹ D. Matvienko,¹ S. McOnie,⁴³ K. Miyabayashi,²⁹ H. Miyata,³⁴ Y. Miyazaki,²⁷ R. Mizuk,¹⁴ G. B. Mohanty,⁴⁴ T. Mori,²⁷ N. Muramatsu,³⁹ E. Nakano,³⁶ M. Nakao,⁹ H. Nakazawa,⁵⁶ S. Neubauer,¹⁷ S. Nishida,⁹ K. Nishimura,⁸ O. Nitoh,⁵² S. Ogawa,⁴⁶ T. Ohshima,²⁷ S. Okuno,¹⁶ S. L. Olsen,^{41,8} Y. Onuki,⁴⁹ H. Ozaki,⁹ P. Pakhlov,¹⁴ G. Pakhlova,¹⁴ H. K. Park,²⁰ K. S. Park,⁴² T. K. Pedlar,²³ R. Pestotnik,¹⁵ M. Petrič,¹⁵ L. E. Piilonen,⁵³ A. Poluektov,¹ M. Röhrken,¹⁷ M. Rozanska,³² H. Sahoo,⁸ K. Sakai,⁹ Y. Sakai,⁹ T. Sanuki,⁴⁸ Y. Sato,⁴⁸ O. Schneider,²¹ C. Schwanda,¹² A. J. Schwartz,³ K. Senyo,⁵⁴ V. Shebalin,¹ C. P. Shen,²⁷ T.-A. Shibata,⁵⁰ J.-G. Shiu,³¹ B. Shwartz,¹ A. Sibidanov,⁴³ F. Simon,^{25,45} J. B. Singh,³⁸ P. Smerkol,¹⁵ Y.-S. Sohn,⁵⁵ A. Sokolov,¹³ E. Solovieva,¹⁴ S. Stanič,³⁵ M. Starič,¹⁵ M. Sumihama,⁵ K. Sumisawa,⁹ T. Sumiyoshi,⁵¹ S. Tanaka,⁹ G. Tatishvili,³⁷ Y. Teramoto,³⁶ I. Tikhomirov,¹⁴ K. Trabelsi,⁹ T. Tsuboyama,⁹ M. Uchida,⁵⁰ S. Uehara,⁹ T. Uglov,¹⁴ Y. Unno,⁷ S. Uno,⁹ Y. Ushiroda,⁹ S. E. Vahsen,⁸ G. Varner,⁸ K. E. Varvell,⁴³ A. Vinokurova,¹ V. Vorobyev,¹ C. H. Wang,³⁰ M.-Z. Wang,³¹ P. Wang,¹¹ M. Watanabe,³⁴ Y. Watanabe,¹⁶ K. M. Williams,⁵³ E. Won,¹⁹ B. D. Yabsley,⁴³ H. Yamamoto,⁴⁸ Y. Yamashita,³³ M. Yamauchi,⁹ Y. Yusa,³⁴ Z. P. Zhang,⁴⁰ V. Zhilich,¹ A. Zupanc,¹⁷ and O. Zyukova¹

(The Belle Collaboration)

¹*Budker Institute of Nuclear Physics SB RAS and Novosibirsk State University, Novosibirsk 630090*

²*Faculty of Mathematics and Physics, Charles University, Prague*

³*University of Cincinnati, Cincinnati, Ohio 45221*

⁴*Justus-Liebig-Universität Gießen, Gießen*

⁵*Gifu University, Gifu*

⁶*Gyeongsang National University, Chinju*

⁷*Hanyang University, Seoul*

⁸*University of Hawaii, Honolulu, Hawaii 96822*

⁹*High Energy Accelerator Research Organization (KEK), Tsukuba*

¹⁰*Indian Institute of Technology Guwahati, Guwahati*

¹¹*Institute of High Energy Physics, Chinese Academy of Sciences, Beijing*

¹²*Institute of High Energy Physics, Vienna*

¹³*Institute of High Energy Physics, Protvino*

¹⁴*Institute for Theoretical and Experimental Physics, Moscow*

¹⁵*J. Stefan Institute, Ljubljana*

¹⁶*Kanagawa University, Yokohama*

¹⁷*Institut für Experimentelle Kernphysik, Karlsruher Institut für Technologie, Karlsruhe*

¹⁸*Korea Institute of Science and Technology Information, Daejeon*

¹⁹*Korea University, Seoul*

²⁰*Kyungpook National University, Taegu*

²¹*École Polytechnique Fédérale de Lausanne (EPFL), Lausanne*

²²*Faculty of Mathematics and Physics, University of Ljubljana, Ljubljana*

²³*Luther College, Decorah, Iowa 52101*

²⁴*University of Maribor, Maribor*

²⁵*Max-Planck-Institut für Physik, München*

²⁶*University of Melbourne, School of Physics, Victoria 3010*

²⁷*Graduate School of Science, Nagoya University, Nagoya*

²⁸*Kobayashi-Maskawa Institute, Nagoya University, Nagoya*

²⁹*Nara Women's University, Nara*

- ³⁰National United University, Miao Li
³¹Department of Physics, National Taiwan University, Taipei
³²H. Niewodniczanski Institute of Nuclear Physics, Krakow
³³Nippon Dental University, Niigata
³⁴Niigata University, Niigata
³⁵University of Nova Gorica, Nova Gorica
³⁶Osaka City University, Osaka
³⁷Pacific Northwest National Laboratory, Richland, Washington 99352
³⁸Panjab University, Chandigarh
³⁹Research Center for Nuclear Physics, Osaka University, Osaka
⁴⁰University of Science and Technology of China, Hefei
⁴¹Seoul National University, Seoul
⁴²Sungkyunkwan University, Suwon
⁴³School of Physics, University of Sydney, NSW 2006
⁴⁴Tata Institute of Fundamental Research, Mumbai
⁴⁵Excellence Cluster Universe, Technische Universität München, Garching
⁴⁶Toho University, Funabashi
⁴⁷Tohoku Gakuin University, Tagajo
⁴⁸Tohoku University, Sendai
⁴⁹Department of Physics, University of Tokyo, Tokyo
⁵⁰Tokyo Institute of Technology, Tokyo
⁵¹Tokyo Metropolitan University, Tokyo
⁵²Tokyo University of Agriculture and Technology, Tokyo
⁵³CNP, Virginia Polytechnic Institute and State University, Blacksburg, Virginia 24061
⁵⁴Yamagata University, Yamagata
⁵⁵Yonsei University, Seoul
⁵⁶National Central University, Chung-li
(Received 23 January 2012; published 23 April 2012)

We present a precise measurement of the CP violation parameter $\sin 2\phi_1$ and the direct CP violation parameter \mathcal{A}_f using the final data sample of $772 \times 10^6 B\bar{B}$ pairs collected at the $Y(4S)$ resonance with the Belle detector at the KEKB asymmetric-energy e^+e^- collider. One neutral B meson is reconstructed in a $J/\psi K_S^0$, $\psi(2S)K_S^0$, $\chi_{c1}K_S^0$, or $J/\psi K_L^0$ CP eigenstate and its flavor is identified from the decay products of the accompanying B meson. From the distribution of proper-time intervals between the two B decays, we obtain the following CP violation parameters: $\sin 2\phi_1 = 0.667 \pm 0.023(\text{stat}) \pm 0.012(\text{syst})$ and $\mathcal{A}_f = 0.006 \pm 0.016(\text{stat}) \pm 0.012(\text{syst})$.

DOI: 10.1103/PhysRevLett.108.171802

PACS numbers: 11.30.Er, 12.15.Hh, 13.25.Hw

In the standard model (SM), CP violation in the quark sector is described by the Kobayashi-Maskawa (KM) theory [1] in which the quark-mixing matrix has a single irreducible complex phase that gives rise to all CP -violating asymmetries. In the decay chain $Y(4S) \rightarrow B^0\bar{B}^0 \rightarrow f_{CP}f_{\text{tag}}$, where one of the B mesons decays at time t_{CP} to a CP eigenstate f_{CP} , and the other B meson decays at time t_{tag} to a final state f_{tag} that distinguishes between B^0 and \bar{B}^0 , the decay rate has a time dependence in the $Y(4S)$ rest frame [2] given by

$$\mathcal{P}(\Delta t) = \frac{e^{-|\Delta t|/\tau_{B^0}}}{4\tau_{B^0}} \{1 + q[\mathcal{S}_f \sin(\Delta m_d \Delta t) + \mathcal{A}_f \cos(\Delta m_d \Delta t)]\}. \quad (1)$$

Here \mathcal{S}_f and \mathcal{A}_f are CP violation parameters, τ_{B^0} is the B^0 lifetime, Δm_d is the mass difference between the two neutral B mass eigenstates, $\Delta t \equiv t_{CP} - t_{\text{tag}}$, and the b -flavor charge $q = +1(-1)$ when the tagging B meson

is a B^0 (\bar{B}^0). With very small theoretical uncertainty [2], the SM predicts $\mathcal{S}_f = -\xi_f \sin 2\phi_1$ and $\mathcal{A}_f = 0$ for the $b \rightarrow c\bar{c}s$ transition, where $\xi_f = +1(-1)$ corresponds to CP -even (-odd) final states and ϕ_1 is an interior angle of the KM unitarity triangle, defined as $\phi_1 \equiv \arg[-V_{cd}V_{cb}^*/V_{td}V_{tb}^*]$ [3]. The BABAR and Belle Collaborations have published several determinations of $\sin 2\phi_1$ since the first observation [4,5]; previous results used 465×10^6 [6] and 535×10^6 [7] $B\bar{B}$ pairs, respectively.

With recently available experimental results, not only $\sin 2\phi_1$ but also other measurements of the sides of the unitarity triangle and other CP violation measurements make it possible to test the consistency of the KM scheme. The indirect determination of the angle ϕ_1 deviates by 2.7σ from the current world average for the direct determination of $\sin 2\phi_1$ [8]. Equivalently, the $B^\pm \rightarrow \tau^\pm \nu_\tau$ branching fraction and the resulting value of $|V_{ub}|$ differ by 2.8σ from the prediction of the global fit [8], where the

$\sin 2\phi_1$ value gives the most stringent constraint on the indirect measurement. Furthermore, time-dependent CP violation in the neutral B meson decays mediated by flavor-changing $b \rightarrow s$ transitions may deviate from CP violation in the $b \rightarrow c\bar{c}s$ case because of possible additional quantum loops [9]. To clarify whether new physics contributes to CP -violating phenomena or $B^\pm \rightarrow \tau^\pm \nu_\tau$ decays, it is very important to determine $\sin 2\phi_1$, the SM reference, as precisely as possible.

In this Letter, we describe the final Belle measurement of $\sin 2\phi_1$ and \mathcal{A}_f in $b \rightarrow c\bar{c}s$ induced B decays to f_{CP} . The B decays to the CP -odd eigenstates, $f_{CP} = J/\psi K_S^0$, $\psi(2S)K_S^0$, and $\chi_{c1}K_S^0$, and the CP -even eigenstate, $f_{CP} = J/\psi K_L^0$, are reconstructed using $772 \times 10^6 B\bar{B}$ pairs, the entire data sample accumulated on the $Y(4S)$ resonance with the Belle detector [10] at the KEKB asymmetric-energy e^+e^- collider [11]. Two inner detector configurations were used. A 2.0 cm radius beam pipe and a 3-layer silicon vertex detector (SVD) were used for the first data sample that contains $152 \times 10^6 B\bar{B}$ pairs. The remaining $620 \times 10^6 B\bar{B}$ pairs were accumulated with a 1.5 cm radius beam pipe, a 4-layer silicon vertex detector, and a small-cell inner drift chamber. The latter data sample has been recently reprocessed using a new charged track reconstruction algorithm, which significantly increased the reconstruction efficiency for the $B^0 \rightarrow (c\bar{c})K_S^0$ decay modes. In particular, the gain for the $B^0 \rightarrow J/\psi K_S^0$ decay mode is 18%.

The $Y(4S)$ is produced with a Lorentz boost of $\beta\gamma = 0.425$ nearly along the z axis, which is antiparallel to the positron beam direction. Since the B^0 and \bar{B}^0 mesons are approximately at rest in the $Y(4S)$ center-of-mass (c.m.) system, Δt can be determined from the displacement in z between the f_{CP} and f_{tag} decay vertices: $\Delta t \simeq (z_{CP} - z_{\text{tag}})/(\beta\gamma c) \equiv \Delta z/(\beta\gamma c)$.

Charged tracks reconstructed in the central drift chamber (CDC), except for tracks from $K_S^0 \rightarrow \pi^+\pi^-$ decays, are required to originate from the interaction point (IP). We distinguish charged kaons from pions based on a kaon (pion) likelihood $\mathcal{L}_{K(\pi)}$ derived from the time-of-flight scintillation counters, aerogel threshold Cherenkov counters, and dE/dx measurements in the CDC. Electron identification is based on the ratio of the electromagnetic calorimeter (ECL) cluster energy to the particle momentum as well as a combination of dE/dx measurements in the CDC, the aerogel threshold Cherenkov counter response, and the position and shape of the electromagnetic shower. Muons are identified by track penetration depth and hit scatter in the muon detector (KLM). Photons are identified as isolated ECL clusters that are not matched to any charged track.

For the $J/\psi K_S^0$, $J/\psi K_L^0$, and $\psi(2S)K_S^0$ modes, event selection is the same as in our previous analyses [7,12], where J/ψ mesons are reconstructed via their decays to $\ell^+\ell^-$ ($\ell = e, \mu$) and the $\psi(2S)$ mesons to $\ell^+\ell^-$ or

$J/\psi \pi^+\pi^-$. For the modes $J/\psi K_L^0$ and $\chi_{c1}K_S^0$, in which the χ_{c1} is reconstructed in the $J/\psi \gamma$ final state, both J/ψ daughter tracks must be positively identified as leptons, whereas for the $J/\psi K_S^0$ and $\psi(2S)K_S^0$ modes, at least one daughter must satisfy this requirement. Any other track having an ECL energy deposit consistent with a minimum ionizing particle is accepted as a muon candidate and any track satisfying either the dE/dx or the ECL shower energy requirements is retained as an electron candidate. For $J/\psi \rightarrow e^+e^-$ decays, the e^\pm charmonium daughters are combined with photons found within 50 mrad of the e^+ or e^- direction in order to account partially for final-state radiation and bremsstrahlung. In order to accommodate the remaining radiative tails, an asymmetric invariant mass requirement is used to select J/ψ and $\psi(2S)$ decays in dilepton modes, $-150 \text{ MeV}/c^2 < M_{e^+e^-} - M_\psi < 36 \text{ MeV}/c^2$ and $-60 \text{ MeV}/c^2 < M_{\mu^+\mu^-} - M_\psi < 36 \text{ MeV}/c^2$, where M_ψ denotes either the nominal J/ψ or $\psi(2S)$ mass. For $\psi(2S) \rightarrow J/\psi \pi^+\pi^-$ candidates, we require a mass difference of $580 \text{ MeV}/c^2 < M_{\ell^+\ell^-\pi^+\pi^-} - M_{\ell^+\ell^-} < 600 \text{ MeV}/c^2$, and $\chi_{c1} \rightarrow J/\psi \gamma$ candidates are required to have a mass difference of $385.0 \text{ MeV}/c^2 < M_{\ell^+\ell^-\gamma} - M_{\ell^+\ell^-} < 430.5 \text{ MeV}/c^2$. For each charmonium candidate, vertex-constrained and mass-constrained fits are applied to improve its momentum resolution.

Candidate $K_S^0 \rightarrow \pi^+\pi^-$ decays are selected by requirements on their invariant mass, flight length, and consistency between the K_S^0 momentum direction and vertex position. Candidate K_L^0 mesons are selected from ECL and/or KLM hit patterns that are consistent with the presence of a shower induced by a K_L^0 meson. The centroid of the K_L^0 candidate shower is required to be within a 45° cone centered on the K_L^0 direction calculated from the two-body B decay kinematics and the momentum of the reconstructed J/ψ meson.

For $B \rightarrow f_{CP}$ candidate reconstruction in modes other than $J/\psi K_L^0$, B candidates are identified by two kinematic variables: the energy difference $\Delta E \equiv E_B^* - E_{\text{beam}}^*$ and the beam-energy constrained mass $M_{bc} \equiv \sqrt{(E_{\text{beam}}^*)^2 - (p_B^*)^2}$, where E_{beam}^* is the CM beam energy, and E_B^* (p_B^*) is the CM energy (momentum) of the reconstructed B candidate. The $B^0 \rightarrow J/\psi K_L^0$ candidates are identified by the value of p_B^* calculated using a two-body decay kinematic assumption.

The b flavor of the accompanying B meson is identified from inclusive properties of particles that are not associated with the reconstructed $B^0 \rightarrow f_{CP}$ decay [13]. The tagging information is represented by two parameters, the b -flavor charge q and purity r . The parameter r is an event-by-event, MC-determined flavor-tagging dilution factor that ranges from $r = 0$ for no flavor discrimination to $r = 1$ for unambiguous flavor assignment. The data are sorted into seven intervals of r . For events with $r > 0.1$, the wrong-tag fractions for six r intervals, w_l ($l = 1, 6$), and their differences between B^0 and \bar{B}^0 decays, Δw_l , are

determined from semileptonic and hadronic $b \rightarrow c$ decays [12,14]. If $r \leq 0.1$, the wrong-tag fraction is set to 0.5, and therefore the tagging information is not used. The total effective tagging efficiency, $\Sigma(f_l \times (1 - 2w_l)^2)$, is determined to be 0.298 ± 0.004 , where f_l is the fraction of events in the category l .

The vertex position for the f_{CP} decay is reconstructed using J/ψ or $\psi(2S)$ daughter tracks that have a minimum number of SVD hits, while the f_{tag} vertex is determined from well-reconstructed tracks that are not assigned to f_{CP} [14]. A constraint on the IP profile in the plane perpendicular to the z axis is used with the selected tracks. With this procedure, we are able to determine a vertex even in the case where only one track has sufficient associated SVD hits. The fractions of the single track vertices for f_{CP} and f_{tag} are about 12% and 23%, respectively.

For a single track vertex, the estimated error of the z coordinate, σ_z , is the indicator of the vertex fit quality and is required to be less than $500 \mu\text{m}$. On the other hand, a vertex reconstructed using two or more tracks is characterized by a more robust goodness-of-fit indicator. In the previous analysis [7], the value of χ^2 of the vertex calculated solely along the z direction was used. This is now replaced by h , the value of χ^2 in three-dimensional space calculated using the charged tracks *without* using the interaction-region profile's constraint [15]. A detailed MC study indicates that h is a superior indicator of the vertex goodness-of-fit because it is less sensitive to the specific B decay mode; in particular, h shows a smaller mode dependence for the vertices reconstructed from $B \rightarrow J/\psi X$ and $B \rightarrow D^{(*)}X$ decays, which are used as control samples to determine the vertex resolution parameters. In the multiple-track vertex case, $h < 50$ and $\sigma_z < 200 \mu\text{m}$ are required. For candidate events in which both B vertices are reconstructed, we retain only those events where the B vertices satisfy $|\Delta t| < 70 \text{ ps}$ for further analysis.

For the candidate events in which both flavor tagging and vertex reconstruction succeed, the signal yield and purity for each mode are obtained from an unbinned maximum-likelihood fit to the two-dimensional $\Delta E - M_{bc}$ distribution for f_{CP} modes with a K_S^0 meson, and to the p_B^* distribution for $J/\psi K_L^0$. The background mainly comes from $B\bar{B}$ events in which one of the B meson decays into a final state containing a correctly reconstructed J/ψ , i.e., the $B \rightarrow J/\psi X$ process. In order to determine this background distribution, a $B \rightarrow J/\psi X$ MC sample corresponding to 100 times the integrated luminosity of data is used. An estimate of other combinatorial backgrounds is obtained from the $M_{\ell^+ \ell^-}$ sideband. For CP -odd modes, the signal distribution is modeled with a Gaussian function in M_{bc} and a double Gaussian function in ΔE . The fits to determine signal yields for these modes are performed in the region $5.2 \text{ GeV}/c^2 < M_{bc} < 5.3 \text{ GeV}/c^2$ and $-0.1 \text{ GeV} < \Delta E < 0.2 \text{ GeV}$. The p_B^* signal shape for $J/\psi K_L^0$ is determined from MC events. The requirement

$p_B^* < 2.0 \text{ GeV}/c$ is used in the fit to estimate the signal yield as well as the contribution of three categories of background: those with a real (those that are correctly reconstructed) J/ψ and a real K_L^0 , those with a real J/ψ and a fake K_L^0 (those that are incorrectly reconstructed from electronic noise or electromagnetic showers), and events with a fake J/ψ (those that are background combinations). The M_{bc} distribution for a stringent ΔE requirement ($|\Delta E| < 40 \text{ MeV}$ for $J/\psi K_S^0$, $|\Delta E| < 30 \text{ MeV}$ for $\psi(2S)K_S^0$, and $|\Delta E| < 25 \text{ MeV}$ for $\chi_{c1}K_S^0$) as well as the p_B^* distribution for $J/\psi K_L^0$ candidates are shown in Fig. 1. We require $5.27 \text{ GeV}/c^2 < M_{bc} < 5.29 \text{ GeV}/c^2$ for f_{CP} modes with a K_S^0 and $0.20 \text{ GeV}/c < p_B^* < 0.45 \text{ GeV}/c$ for $J/\psi K_L^0$ for the fit to the CP violation parameters. For the candidates passing all the criteria mentioned above, the signal yield and purity are estimated for each CP eigenstate and are listed in Table I.

We determine S_f and \mathcal{A}_f for each mode by performing an unbinned maximum-likelihood fit to the observed Δt distribution. The probability density function (PDF) for the signal distribution, $\mathcal{P}_{\text{sig}}(\Delta t; S_f, \mathcal{A}_f, q, w_l, \Delta w_l)$, is given by Eq. (1), fixing τ_{B^0} and Δm_d at their world average values [16] and including modifications to take the effect of an incorrect flavor assignment (parametrized by w_l and Δw_l) into account. The distribution is convolved with the proper-time interval resolution function, $R_{\text{sig}}(\Delta t)$, formed by convolving four components: the detector resolutions for z_{CP} and z_{tag} , the shift of the z_{tag} vertex position due to secondary tracks from charmed particle decays, and the kinematic approximation that the B mesons are at rest in the CM frame [17]. Because we now use h to characterize the vertex goodness of fit, each of these resolution function components in Ref. [17] is reformulated as a function of h and σ_z .

Using the M_{bc} sideband events, the background PDF, $\mathcal{P}_{\text{bkg}}(\Delta t)$, for each of the CP -odd modes is modeled as a

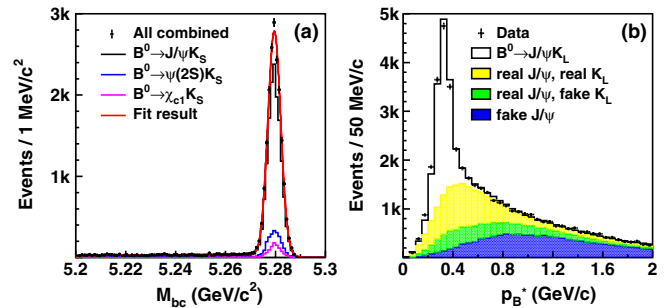


FIG. 1 (color online). (a) M_{bc} distribution within the ΔE signal region for $B^0 \rightarrow J/\psi K_S^0$ (black), $\psi(2S)K_S^0$ (blue), and $\chi_{c1}K_S^0$ (magenta); the superimposed curve (red) shows the combined fit result for all these modes. (b) p_B^* distribution of $B^0 \rightarrow J/\psi K_L^0$ candidates with the results of the fit separately indicated as signal (open histogram), background with a real J/ψ and real K_L^0 's (yellow), with a real J/ψ and a fake K_L^0 candidate (green), and with a fake J/ψ (blue).

TABLE I. CP eigenvalue (ξ_f), signal yield (N_{sig}), and purity for each $B^0 \rightarrow f_{CP}$ mode.

Decay mode	ξ_f	N_{sig}	Purity (%)
$J/\psi K_S^0$	-1	12649 ± 114	97
$\psi(2S)(\ell^+\ell^-)K_S^0$	-1	904 ± 31	92
$\psi(2S)(J/\psi\pi^+\pi^-)K_S^0$	-1	1067 ± 33	90
$\chi_{c1}K_S^0$	-1	940 ± 33	86
$J/\psi K_L^0$	+1	10040 ± 154	63

sum of exponential and prompt components, and is convolved with $R_{\text{bkg}}(\Delta t)$ expressed as a double Gaussian function. In the $J/\psi K_L^0$ mode, there are CP violating modes among the $B \rightarrow J/\psi X$ backgrounds, which are included in the background PDF. The Δt PDFs for the remaining $B \rightarrow J/\psi X$ and other combinatorial backgrounds are estimated from the corresponding large MC sample and $M_{\ell^+\ell^-}$ sideband events, respectively. The construction of these PDFs follows the same procedure as in our previous analyses [7,12].

We determine the following likelihood for the i th event:

$$P_i = (1 - f_{\text{ol}}) \sum_k f_k \int [\mathcal{P}_k(\Delta t') R_k(\Delta t_i - \Delta t')] d(\Delta t') + f_{\text{ol}} P_{\text{ol}}(\Delta t_i), \quad (2)$$

where the index k labels each signal or background component. The fraction f_k depends on the r region and is calculated on an event-by-event basis as a function of ΔE and M_{bc} for the CP -odd modes and p_B^* for the CP -even mode. The term $P_{\text{ol}}(\Delta t)$ is a broad Gaussian function that represents an outlier component f_{ol} , which has a fractional normalization of order 0.5% [17]. The only free parameters in the fits are \mathcal{S}_f and \mathcal{A}_f , which are determined by maximizing the likelihood function $L = \prod_i P_i(\Delta t_i; \mathcal{S}_f, \mathcal{A}_f)$. This likelihood is maximized for each f_{CP} mode individually, as well as for all modes combined taking into account their CP -eigenstate values; the results are shown in Table II. Figure 2 shows the Δt distributions and asymmetries for good tag quality ($r > 0.5$) events. We define the background-subtracted asymmetry in each Δt bin by

TABLE II. CP violation parameters for each $B^0 \rightarrow f_{CP}$ mode and from the simultaneous fit for all modes together. The first and second errors are statistical and systematic uncertainties, respectively.

Decay mode	$\sin 2\phi_1 \equiv -\xi_f \mathcal{S}_f$	\mathcal{A}_f
$J/\psi K_S^0$	$+0.670 \pm 0.029 \pm 0.013$	$-0.015 \pm 0.021^{+0.045}_{-0.023}$
$\psi(2S)K_S^0$	$+0.738 \pm 0.079 \pm 0.036$	$+0.104 \pm 0.055^{+0.047}_{-0.027}$
$\chi_{c1}K_S^0$	$+0.640 \pm 0.117 \pm 0.040$	$-0.017 \pm 0.083^{+0.046}_{-0.026}$
$J/\psi K_L^0$	$+0.642 \pm 0.047 \pm 0.021$	$+0.019 \pm 0.026^{+0.017}_{-0.041}$
All modes	$+0.667 \pm 0.023 \pm 0.012$	$+0.006 \pm 0.016 \pm 0.012$

$(N_+ - N_-)/(N_+ + N_-)$, where $N_+(N_-)$ is the signal yield with $q = +1(-1)$.

Uncertainties originating from the vertex reconstruction algorithm are a significant part of the systematic error for both $\sin 2\phi_1$ and \mathcal{A}_f . These uncertainties are reduced by almost a factor of 2 compared to the previous analysis [7] by using h for the vertex-reconstruction goodness-of-fit parameter, as described above. In particular, the effect of the vertex quality cut is estimated by changing the requirement to either $h < 25$ or $h < 100$; the systematic error due to the IP constraint in the vertex reconstruction is estimated by varying the IP profile size in the plane perpendicular to the z axis; the effect of the criterion for the selection of tracks used in the f_{tag} vertex is estimated by changing the requirement on the distance of the closest approach with respect to the reconstructed vertex by $\pm 100 \mu\text{m}$ from the nominal maximum value of $500 \mu\text{m}$. Systematic errors due to imperfect SVD alignment are estimated from MC samples that have artificial misalignment effects. Small biases in the Δz measurement are observed in $e^+e^- \rightarrow \mu^+\mu^-$ and other control samples: To account for these, a special correction function is applied and the variation with respect to the nominal results is included as a systematic error. We also vary the $|\Delta t|$ range by ± 30 ps to estimate the systematic uncertainty due to the $|\Delta t|$ fit range. The vertex resolution function is another major source of $\sin 2\phi_1$ and \mathcal{A}_f uncertainty. This effect is estimated by varying each resolution function parameter obtained from data (MC) by $\pm 1\sigma$ ($\pm 2\sigma$) and repeating the fit to add each variation in quadrature. The uncertainty in the estimated errors of the parameters of reconstructed charged tracks is also taken into account. The largest contribution to the

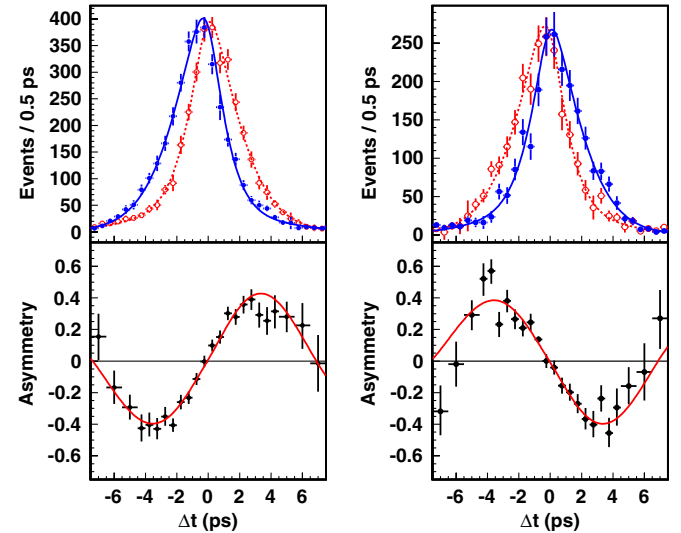


FIG. 2 (color online). The background-subtracted Δt distribution (top) for $q = +1$ (red) and $q = -1$ (blue) events and asymmetry (bottom) for good tag quality ($r > 0.5$) events for all CP -odd modes combined (left) and the CP -even mode (right).

TABLE III. Systematic errors in \mathcal{S}_f and \mathcal{A}_f in each f_{CP} mode and for the sum of all modes.

		$J/\psi K_S^0$	$\psi(2S)K_S^0$	$\chi_{c1}K_S^0$	$J/\psi K_L^0$	All
Vertexing	\mathcal{S}_f	± 0.008	± 0.031	± 0.025	± 0.011	± 0.007
	\mathcal{A}_f	± 0.022	± 0.026	± 0.021	± 0.015	± 0.007
Δt resolution	\mathcal{S}_f	± 0.007	± 0.007	± 0.005	± 0.007	± 0.007
	\mathcal{A}_f	± 0.004	± 0.003	± 0.004	± 0.003	± 0.001
Tag-side interference	\mathcal{S}_f	± 0.002	± 0.002	± 0.002	± 0.001	± 0.001
	\mathcal{A}_f	$^{+0.038}_{-0.000}$	$^{+0.038}_{-0.000}$	$^{+0.038}_{-0.000}$	$^{+0.000}_{-0.037}$	± 0.008
Flavor tagging	\mathcal{S}_f	± 0.003	± 0.003	± 0.004	± 0.003	± 0.004
	\mathcal{A}_f	± 0.003	± 0.003	± 0.003	± 0.003	± 0.003
Possible fit bias	\mathcal{S}_f	± 0.004	± 0.004	± 0.004	± 0.004	± 0.004
	\mathcal{A}_f	± 0.005	± 0.005	± 0.005	± 0.005	± 0.005
Signal fraction	\mathcal{S}_f	± 0.004	± 0.016	< 0.001	± 0.016	± 0.004
	\mathcal{A}_f	± 0.002	± 0.006	< 0.001	± 0.006	± 0.002
Background Δt PDFs	\mathcal{S}_f	< 0.001	± 0.002	± 0.030	± 0.002	± 0.001
	\mathcal{A}_f	< 0.001	< 0.001	± 0.014	< 0.001	< 0.001
Physics parameters	\mathcal{S}_f	± 0.001	± 0.001	± 0.001	± 0.001	± 0.001
	\mathcal{A}_f	< 0.001	< 0.001	± 0.001	< 0.001	< 0.001
Total	\mathcal{S}_f	± 0.013	± 0.036	± 0.040	± 0.021	± 0.012
	\mathcal{A}_f	$^{+0.045}_{-0.023}$	$^{+0.047}_{-0.027}$	$^{+0.046}_{-0.026}$	$^{+0.017}_{-0.041}$	± 0.012

systematic uncertainty in \mathcal{A}_f is the effect of the tag-side interference (TSI), which is described in detail in [18]. Since the effect of TSI has an opposite sign for different CP eigenstates, there is a partial cancellation in the combined result. Hence, the combined TSI systematic is smaller than the systematic in each individual mode. Systematic errors due to uncertainties in the wrong-tag fractions are studied by varying the wrong-tag fraction individually in each r region. A possible fit bias is examined by fitting a large number of MC events. Other contributions come from uncertainties in the signal fractions, the background Δt distribution, τ_{B^0} , and Δm_d . Each contribution is summarized in Table III. We add them in quadrature to obtain the total systematic uncertainty.

In summary, we present the final $\sin 2\phi_1$ measurement using the entire Belle $Y(4S)$ data sample containing $772 \times 10^6 B\bar{B}$ pairs. We have reconstructed $b \rightarrow c\bar{c}s$ induced B meson decays in three CP -odd modes [$J/\psi K_S^0$, $\psi(2S)K_S^0$, and $\chi_{c1}K_S^0$] and one CP -even mode ($J/\psi K_L^0$). The fit, using common CP -sensitive parameters for all four modes, yields the values $\sin 2\phi_1 = 0.667 \pm 0.023(\text{stat}) \pm 0.012(\text{syst})$ and $\mathcal{A}_f = 0.006 \pm 0.016(\text{stat}) \pm 0.012(\text{syst})$. The results are consistent with previous measurements [6,7]. These are the most precise determinations of these parameters and solidify the SM reference value used to test for evidence of new physics beyond the SM.

We thank the KEKB group for excellent operation of the accelerator; the KEK cryogenics group for efficient solenoid operations; and the KEK computer group, the NII, and PNNL/EMSL for valuable computing and SINET4 network support. We acknowledge support from MEXT, JSPS and Nagoya's TLPRC (Japan); ARC and DIISR (Australia); NSFC (China); MSMT (Czechia); DST (India); INFN (Italy); MEST, NRF, GSDC of KISTI, and

WCU (Korea); MNiSW (Poland); MES and RFAAE (Russia); ARRS (Slovenia); SNSF (Switzerland); NSC and MOE (Taiwan); and DOE and NSF (U.S.).

- [1] M. Kobayashi and T. Maskawa, *Prog. Theor. Phys.* **49**, 652 (1973).
- [2] A. B. Carter and A. I. Sanda, *Phys. Rev. D* **23**, 1567 (1981); I. I. Bigi and A. I. Sanda, *Nucl. Phys.* **B193**, 85 (1981).
- [3] Another naming convention $\beta(\equiv \phi_1)$ is also used in the literature.
- [4] B. Aubert *et al.* (BABAR Collaboration), *Phys. Rev. Lett.* **87**, 091801 (2001).
- [5] K. Abe *et al.* (Belle Collaboration), *Phys. Rev. Lett.* **87**, 091802 (2001).
- [6] B. Aubert *et al.* (BABAR Collaboration), *Phys. Rev. D* **79**, 072009 (2009).
- [7] K. F. Chen *et al.* (Belle Collaboration), *Phys. Rev. Lett.* **98**, 031802 (2007).
- [8] J. Charles *et al.* (CKMfitter Group), *Phys. Rev. D* **84**, 033005 (2011).
- [9] Y. Grossman and M. P. Worah, *Phys. Lett. B* **395**, 241 (1997); D. London and A. Soni, *Phys. Lett. B* **407**, 61 (1997); T. Moroi, *Phys. Lett. B* **493**, 366 (2000); D. Chang, A. Masiero and H. Murayama, *Phys. Rev. D* **67**, 075013 (2003); S. Baek, T. Goto, Y. Okada, and K. I. Okumura, *Phys. Rev. D* **64**, 095001 (2001).
- [10] A. Abashian *et al.* (Belle Collaboration), *Nucl. Instrum. Methods Phys. Res., Sect. A* **479**, 117 (2002).
- [11] S. Kurokawa and E. Kikutani, *Nucl. Instrum. Methods Phys. Res., Sect. A* **499**, 1 (2003), and other papers included in this volume.
- [12] K. Abe *et al.* (Belle Collaboration), *Phys. Rev. D* **71**, 072003 (2005); H. Sahoo *et al.* (Belle Collaboration), *Phys. Rev. D* **77**, 091103 (2008).

-
- [13] H. Kakuno *et al.*, *Nucl. Instrum. Methods Phys. Res., Sect. A* **533**, 516 (2004).
- [14] K. F. Chen *et al.* (Belle Collaboration), *Phys. Rev. D* **72**, 012004 (2005).
- [15] Details of the vertex fit and the parametrization of the resolution function are given in an accompanying Phys. Rev. D paper (in preparation).
- [16] K. Nakamura *et al.* (Particle Data Group), *J. Phys. G* **37**, 075021 (2010).
- [17] H. Tajima *et al.*, *Nucl. Instrum. Methods Phys. Res., Sect. A* **533**, 370 (2004).
- [18] O. Long, M. Baak, R. N. Cahn, and D. Kirkby, *Phys. Rev. D* **68**, 034010 (2003).